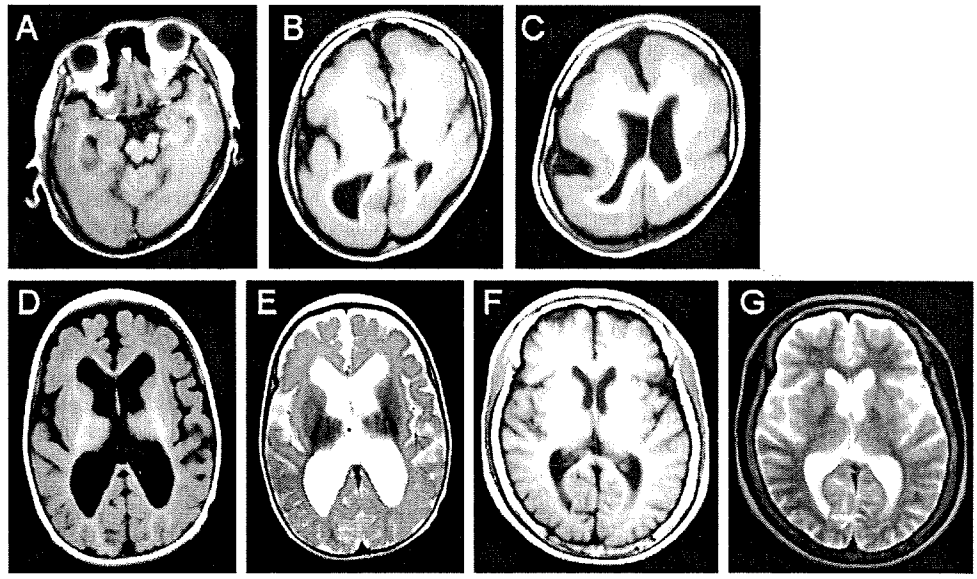

Q2 Figure 1 aCGH analysis of the 17p13.3 region in 3 epilepsy patients and a corresponding genetic map of the MDS region. Genomic copy number aberrations were identified in 3 patients by CGH Analytics software. The horizontal and vertical axes indicate the position along 17p13.3 and the $\log_2$ ratio of the genomic copy number, respectively. The gray rectangles indicate regions of copy number aberrations. The dots indicate the annealing locations and the corresponding $\log_2$ ratios for each probe. The black dots indicate normal $\log_2$ ratio; whereas, red and green indicate $\log_2$ ratio higher than 0.5 and lower than −0.5, respectively. The red and black rectangles indicate locations of the previously reported CNVs and the known genes in the indicated regions. The names of the known genes are indicated below the figure, and YWHAE, CRK, and LIS1 are highlighted in bold. (For interpretation of the references to color in this figure caption, the reader is referred to the web version of the article.)

In patient 2, a gain of genomic copy number was identified by aCGH in the MDS region containing LIS1 (Fig. 1). The mean $\log_2$ signal ratios were +0.5 in chr17 (1,899,328–2,151,328) and +1 in chr17 (2,165,727–3,065,623), indicating duplication and triplication, respectively. These aberrations were confirmed by FISH analysis (Fig. 2B and Table 1), and fiber-FISH analyses revealed the directions of all triplicated segments with tandem insertions (Fig. 2D). The fact that neither parent of patient 2 showed any signal abnormalities in FISH analysis (data not shown) confirmed the de novo triplication in patient 2.

Figure 2 FISH and fiber-FISH analysis of the 3 patients. (A) Patient 1: partial deletion of LIS1 was identified. The arrows indicate markers of chromosome 17 (RP11-1D5; red), and the arrowhead indicates the originally constructed partial sequence of LIS1 (green). (B) Patient 2: duplication of LIS1 was identified. FISH analysis indicated a predominant LIS1 signal (RP11-135N5; green) in one allele of chromosome 17 (arrow) and increased LIS1 signal numbers in metaphase (arrowhead). The red signals indicate markers, RP11-1D5. (C) Patient 3: one allele of YWHAE (RP11-356I18; green) is deleted (arrowhead). The red signals indicate markers, RP11-153A23. (D) Patient 2: fiber-FISH analysis identified a tandem triplication of the LIS1 region in one of the chromosomal fibers. The green signals represent RP11-135N5, and the red signals represent CTD-2576K4. The arrows reflect a single unit of LIS1 staining. The single arrow at the bottom represents a normal chromosome 17. (For interpretation of the references to color in this figure caption, the reader is referred to the web version of the article.)

Please cite this article in press as: Shimojima, K., et al., Genomic copy number variations at 17p13.3 and epileptogenesis. Epilepsy Res. (2010), doi:10.1016/j.eplepsyres.2010.02.002

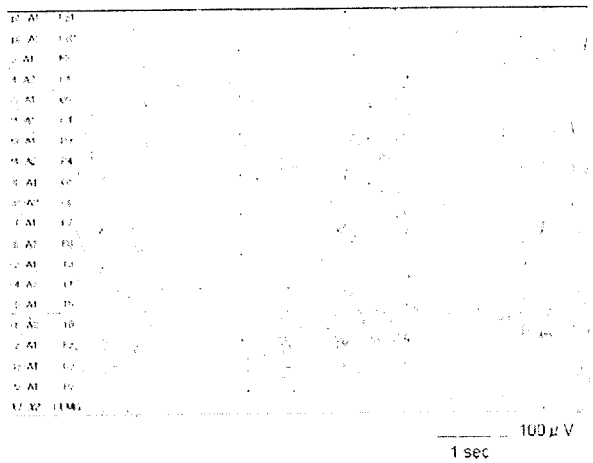

Figure 3 Brain MRI images of the three patients. (A–C) Grade 3 lissencephaly with predominant agyria in the posterior region was seen in patient 1. (D and E) Generalized hypoplasia of the brain involving the cortical and white matter regions was noted in patient 2. (F and G) Mild volume loss of the brain was identified in patient 3. (A–D, F) T1-weighted MRI image. (E and G) T2-weighted MRI image.

In patient 3, aCGH analysis revealed a terminal deletion of 17p, chr17 (1–1,280,058), which included YWHAE and CRK, but not LIS1 (Fig. 1). This was confirmed by FISH analysis (Fig. 2C). The parental samples showed no abnormalities in this region (data not shown), indicating de novo deletion of 17p in patient 3.

Clinical reports

Patient 1 is a 22-year-old female was born at 38 gestational weeks with a weight of 2540 g (<25th centile). Since the patient showed no eye following and no responsive smiles at the age of 5 months, she was admitted to the hospital, and global agyria was identified by brain computed tomography (CT). In infancy, she started to suffer from several types of seizures, most of which were generalized tonic–clonic seizures, and an electroencephalography (EEG) examination showed irregular high-voltage slow waves with continuous multi-focal sharp waves (data not shown). These epileptic seizures were refractory to medical treatment. At the age of 16 years and 7 months, brain magnetic resonance imaging (MRI) analysis revealed lissencephaly with a predominance in the posterior region indicating grade 3 lissencephaly (Fig. 3A–C) (Kato and Dobyns, 2003). She was diagnosed with isolated lissencephaly because of her normal facial features (Fig. 4A). At 22 years of age, she showed good eye contact, visual tracking, social smiling, and various other facial expressions in response to parental vocalization, although she could not speak and had no head control. Epileptic seizures occurred several times a week. She was capable of taking oral paste foods and did not need tube feeding at home. Conventional G-banding chromosomal analysis showed a normal female karyotype (46,XX), and subsequent fluorescent in situ hybridization (FISH) analysis using a commercially available probe, the Vysis Miller-Dieker Region/Isolated Lissencephaly Probe LSI LIS1 (Abbott Laboratories, Abbott Park, IL, USA), indicated no deletion at 17p13.3 (data not shown).

Patient 2 is an 11-month-old girl was referred to us for infantile spasms. She was born at 39 weeks gestation with a birth weight of 1992 g (<3rd centile). At 6 months, her first epileptic seizure with deviation of eye position was noted, and EEG analysis showed modified hypsarrhythmia with synchronized high-voltage slow waves indicating West syndrome (Fig. 5). A subsequent brain MRI examination revealed generalized hypoplasia of the brain involving the cortical and white matter regions, associated with hypoplasia of the corpus callosum, which resulted in ventricular dilatation (Fig. 3C). Although several orally administered anti-epileptic drugs were ineffective, subsequent adrenocorticotropic hormone (ACTH) therapy was effective. At 6 months, she lacked neck control and could not roll over due to severe hypotonia. Conventional G-banding showed a normal female karyotype. At the age of 21 months, patient 2 showed an average growth rate with her length of 83.5 cm (=50th centile), weight of 10.0 kg (=50th centile), and head circumference of 47.0 cm (=50th centile). At this time, she was able to turn over but could not sit alone, indicating a severe developmental delay.

Patient 3 is a 23-year-old male was born to healthy parents at 39 weeks gestation with a birth weight of 2500 g (<50th centile). Delivery was uneventful. He suffered from mild developmental delay in infancy and from secondary generalized partial seizures at the age of 6 years. Subsequently, he suffered various types of seizures that were refractory to many different anti-epileptic drugs. Communication was challenging for him. At the age of 20 years, the Wechsler Adult Intelligence Scale (WAIS) indicated that his full IQ was 45 (verbal = 59, performance = 45). At the time of the study, he was working at a social welfare institution. His height was 155.5 cm (<3rd centile), his weight was 52.3 kg (<25th centile), and his head circumference was 56.2 cm (<25th centile). He had distinctive facial features (Fig. 4C). Conventional G-banding showed a normal male karyotype of 46,XY. A brain MRI examination revealed mild volume loss of the brain (Fig. 3F and G).

Discussion

In this study, we identified pathogenic CNVs in 17p13.3, the MDS critical region, in 3 epileptic patients.

Patient 1 had isolated grade 3 lissencephaly (Kato and Dobyns, 2003) but lacked the dysmorphic features common among MDS patients. As a commercially available LIS1 probe did not detect deletion, aCGH analysis was performed and identified a microdeletion involving the last 5 exons of LIS1. This was similar to the findings of the previous report, in which FISH analysis using a commercially available LIS1 probe yielded a false-negative result for a patient with a deletion in the 5′ region of LIS1 (Izumi et al., 2007). In both cases, the incorrect analysis resulted from a partial LIS1 deletion and from the limited availability of commercial FISH analysis probes. The deletion region of patient 1 included two other neighboring genes; KIAA0664, which encodes a hypothetical protein, and GARNL4, which encodes a GTPase-activating protein that activates the small guanine-nucleotide-binding protein Rap1 in platelets. Thus,

Please cite this article in press as: Shimojima, K., et al., Genomic copy number variations at 17p13.3 and epileptogenesis. Epilepsy Res. (2010), doi:10.1016/j.eplepsyres.2010.02.002

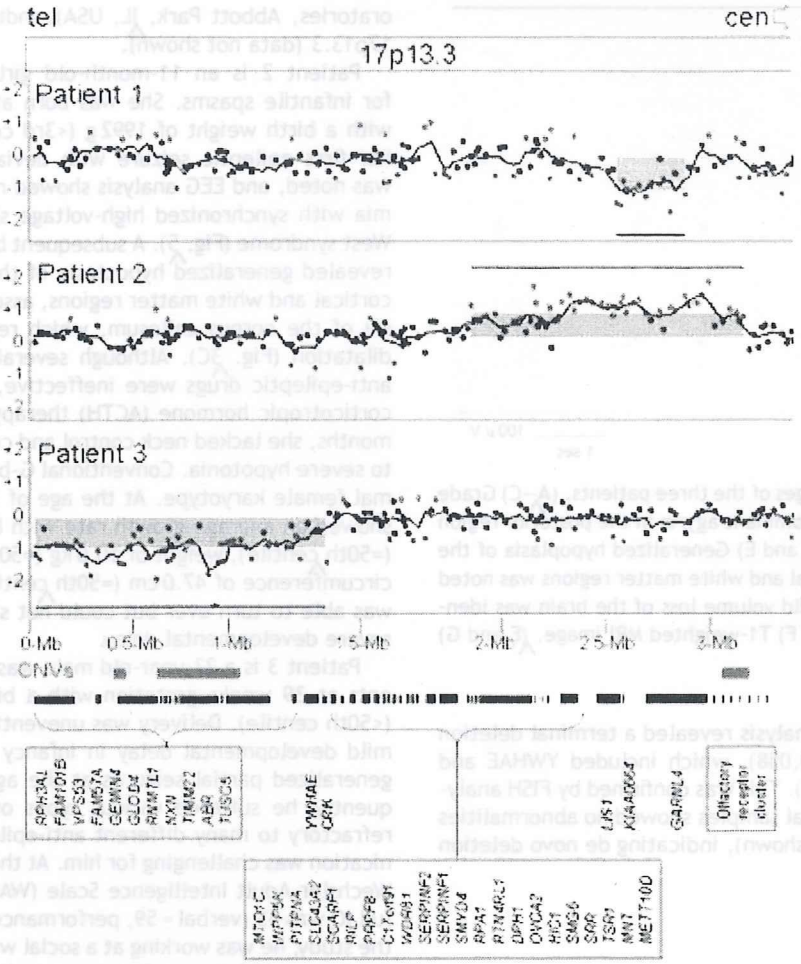

Figure 4 Portraits of the three patients. There were no distinct facial morphologies for patient 1 (A) or patient 2 (B). (C) Patient 3 showed a prominent forehead, bilateral ptosis, a broad nasal root, epicanthal folds, and retrognathia. Signed consent forms authorizing publication of the unmasked images of all identifiable patients have been obtained from the patients and/or their guardians.

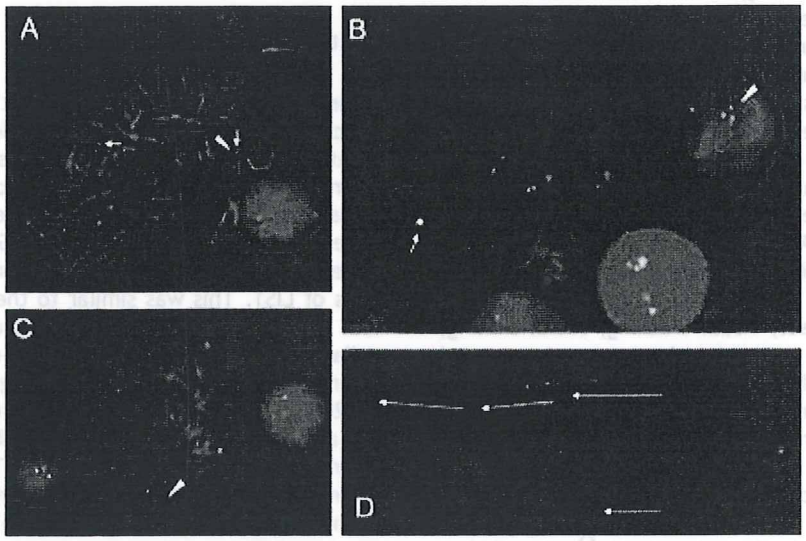

Figure 5 EEG analysis of patient 2, indicating modified hypsarrhythmia.

Please cite this article in press as: Shimojima, K., et al., Genomic copy number variations at 17p13.3 and epileptogenesis. Epilepsy Res. (2010), doi:10.1016/j.eplepsyres.2010.02.002

their detailed functions in the central nervous system are unknown. Patient 1 has shown long-term survival without physical or mental deterioration despite the fact that the majority of patients with lissencephaly die early in childhood (de Rijk-van Andel et al., 1990). In contrast, MDS patients with a large telomeric deletion of 17p13.3 present with a severe phenotype, including lissencephaly; significant facial dysmorphism; and occasionally other congenital visceral anomalies such as gastrointestinal and cardiac defects; and furthermore, the severity of lissencephaly in MDS patients is severer than that seen in cases of isolated lissencephaly (Cardoso et al., 2003; Dobyns et al., 1991).

Mei et al. (2008) analyzed 45 patients with isolated lissencephaly; 44% of the patients (20/45) showed LIS1 mutations, and small deletions/duplications were identified in 76% of the patients without LIS1 mutations (19/25). One of the 19 patients lacking LIS1 mutations exhibited duplication of three LIS1 exons. Haverfield et al. (2009) analyzed 52 patients with lissencephaly, and intragenic duplication of LIS1 was identified in 6 patients. These microduplications will disrupt LIS1 structures and result in loss of function of the LIS1 product. On the other hand, two recent reports described microduplications encompassing the entire LIS1 region 11,13 (Bi et al., 2009; Roos et al., 2009). Using transgenic mice, Bi et al. (2009) confirmed that LIS1/PAFAH1B1 overexpression derived from genomic copy number gain was responsible for abnormal neurodevelopment. They also reported a patient with LIS1 triplication (Subject 6) (Bi et al., 2009). Similarly, we identified a triplication of LIS1 in patient 2, whose MRI demonstrated normal gyrus formation but a reduced cerebral volume. Patient 2 exhibited infantile spasms; whereas, the patient with LIS1 triplication (Subject 6) reported by Bi et al. (2009) lacked seizure activity. This difference may have resulted from the size difference between them, as the triplication size of patient 2 was much larger than that of the patient (Subject 6) reported by Bi et al. (2009). Accordingly, genomic copy number aberrations at 17p13.3 including LIS1 can lead to neurodevelopmental delay and epilepsy regardless of whether the aberration reflects a gain or loss of copy number.

In this study, patient 3 had a complete terminal deletion of 17p, and he demonstrated the dysmorphic facial features and growth retardation associated with mental retardation. This was compatible with a report by Sreenath Nagamani et al. (2009) in which haploinsufficiency of YWHAE and CRK was suggested to be responsible for facial dysmorphism and growth deficiency, respectively. However, in our present study, patient 3 had intractable epilepsy. Among the previously reported patients with a terminal deletion of 17p that did not include LIS1, only 1 patient with der(17)t(5;17)(p13.1;p13.3) was reported to have seizure episodes (Mutchinick et al., 1999).

In conclusion, it was suggested that the identified gain or loss of genomic copy number within 17p13.3 result in epileptogenesis and that triplication of LIS1 can cause symptomatic West syndrome.

Conflict of interest

None of the authors has any conflict of interest to disclosure.

Acknowledgements

This work was supported by the International Research and Educational Institute for Integrated Medical Sciences and the Tokyo Women's Medical University, which is supported by the Program for Promoting the Establishment of Strategic Research Centers; Special Coordination Funds for Promoting Science and Technology; and Ministry of Education, Culture, Sports, Science and Technology (Japan).

Appendix A. Supplementary data

Supplementary data associated with this article can be found, in the online version, at doi:10.1016/j.eplepsyres.2010.02.002.

References

Bi, W., Sapir, T., Shchelochkov, O.A., Zhang, F., Withers, M.A., Hunter, J.V., Levy, T., Shinder, V., Peiffer, D.A., Gunderson, K.L., Nezarati, M.M., Shotts, V.A., Amato, S.S., Savage, S.K., Harris, D.J., Day-Salvatore, D.L., Horner, M., Lu, X.Y., Sahoo, T., Yanagawa, Y., Beaudet, A.L., Cheung, S.W., Martinez, S., Lupski, J.R., Reiner, O., 2009. Increased LIS1 expression affects human and mouse brain development. Nat. Genet. 41, 168–177.

Cardoso, C., Leventer, R.J., Matsumoto, N., Kuc, J.A., Ramocki, M.B., Mewborn, S.K., Dudlicek, L.L., May, L.F., Mills, P.L., Das, S., Pilz, D.T., Dobyns, W.B., Ledbetter, D.H., 2000. The location and type of mutation predict malformation severity in isolated lissencephaly caused by abnormalities within the LIS1 gene. Hum. Mol. Genet. 9, 3019–3028.

Cardoso, C., Leventer, R.J., Ward, H.L., Toyo-Oka, K., Chung, J., Gross, A., Martin, C.L., Allanson, J., Pilz, D.T., Olney, A.H., Mutchinick, O.M., Hirotsune, S., Wynshaw-Boris, A., Dobyns, W.B., Ledbetter, D.H., 2003. Refinement of a 400-kb critical region allows genotypic differentiation between isolated lissencephaly, Miller-Dieker syndrome, and other phenotypes secondary to deletions of 17p13.3. Am. J. Hum. Genet. 72, 918–930.

de Rijk-van Andel, J.F., Arts, W.F., Barth, P.G., Loonen, M.C., 1990. Diagnostic features and clinical signs of 21 patients with lissencephaly type 1. Dev. Med. Child Neurol. 32, 707–717.

Dobyns, W.B., Curry, C.J., Hoyme, H.E., Turlington, L., Ledbetter, D.H., 1991. Clinical and molecular diagnosis of Miller-Dieker syndrome. Am. J. Hum. Genet. 48, 584–594.

Dobyns, W.B., Reiner, O., Carrozzo, R., Ledbetter, D.H., 1993. Lissencephaly. A human brain malformation associated with deletion of the LIS1 gene located at chromosome 17p13. JAMA 270, 2838–2842.

Emanuel, B.S., Saitta, S.C., 2007. From microscopes to microarrays: dissecting recurrent chromosomal rearrangements. Nat. Rev. Genet. 8, 869–883.

Haverfield, E.V., Whited, A.J., Petras, K.S., Dobyns, W.B., Das, S., 2009. Intragenic deletions and duplications of the LIS1 and DCX genes: a major disease-causing mechanism in lissencephaly and subcortical band heterotopia. Eur. J. Hum. Genet. 17, 911–918.

Izumi, K., Kuratsuji, G., Ikeda, K., Takahashi, T., Kosaki, K., 2007. Partial deletion of LIS1: a pitfall in molecular diagnosis of Miller-Dieker syndrome. Pediatr. Neurol. 36, 258–260.

Kato, M., Dobyns, W.B., 2003. Lissencephaly and the molecular basis of neuronal migration. Hum. Mol. Genet., 12 Spec No. 1, R89-96.

Lee, J.A., Lupski, J.R., 2006. Genomic rearrangements and gene copy-number alterations as a cause of nervous system disorders. Neuron 52, 103–121.

Mei, D., Lewis, R., Parrini, E., Lazarou, L.P., Marini, C., Pilz, D.T., Guerrini, R., 2008. High frequency of genomic deletions—and a

Please cite this article in press as: Shimojima, K., et al., Genomic copy number variations at 17p13.3 and epileptogenesis. Epilepsy Res. (2010), doi:10.1016/j.eplepsyres.2010.02.002

duplication—in the LIS1 gene in lissencephaly: implications for molecular diagnosis. J. Med. Genet. 45, 355–361.

Mignon-Ravix, C., Cacciagli, P., El-Waly, B., Moncla, A., Milh, M., Girard, N., Chabrol, B., Philip, N., Villard, L., 2009. Deletion of YWHAE in a patient with periventricular heterotopias and marked corpus callosum hypoplasia. J. Med. Genet. Published online, 26 July 2009, doi:2010.1136/jmg.2009.069112.

Mutchinick, O.M., Shaffer, L.G., Kashork, C.D., Cervantes, E.I., 1999. Miller-Dieker syndrome and trisomy 5p in a child carrying a derivative chromosome with a microdeletion in 17p13.3 telomeric to the LIS1 and the D17S379 loci. Am. J. Med. Genet. 85, 99–104.

Reiner, O., Carrozzo, R., Shen, Y., Wehnert, M., Faustinella, F., Dobyns, W.B., Caskey, C.T., Ledbetter, D.H., 1993. Isolation of a Miller-Dieker lissencephaly gene containing G protein beta-subunit-like repeats. Nature 364, 717–721.

Roos, L., Jonch, A.E., Kjaergaard, S., Taudorf, K., Simonsen, H., Hamborg-Petersen, B., Brondum-Nielsen, K., Kirchhoff, M., 2009. A new microduplication syndrome encompassing the region of the Miller-Dieker (17p13 deletion) syndrome. J. Med. Genet. 46, 703–710.

Shaffer, L.G., Theisen, A., Bejjani, B.A., Ballif, B.C., Aylsworth, A.S., Lim, C., McDonald, M., Ellison, J.W., Kostiner, D., Saitta, S., Shaikh, T., 2007. The discovery of microdeletion syndromes in the post-genomic era: review of the methodology and characterization of a new 1q41q42 microdeletion syndrome. Genet. Med. 9, 607–616.

Shimojima, K., Tanaka, K., Yamamoto, T., 2009. A de novo intrachromosomal tandem duplication at 22q13.1q13.31 including the Rubinstein-Taybi region but with no bipolar disorder. Am. J. Med. Genet. A 149A, 1359–1363.

Sreenath Nagamani, S.C., Zhang, F., Shchelochkov, O.A., Bi, W., Ou, Z., Scaglia, F., Probst, F.J., Shinawi, M., Eng, C., Hunter, J.V., Sparagana, S., Lagoe, E., Fong, C.T., Pearson, M., Doco-Fenzy, M., Landais, E., Mozelle, M., Chinault, A.C., Patel, A., Bacino, C.A., Sahoo, T., Kang, S.H., Cheung, S.W., Lupski, J.R., Stankiewicz, P., 2009. Microdeletions including YWHAE in the Miller-Dieker syndrome region on chromosome 17p13.3 result in facial dysmorphisms, growth restriction, and cognitive impairment. J. Med. Genet. 46, 825–833.

Please cite this article in press as: Shimojima, K., et al., Genomic copy number variations at 17p13.3 and epileptogenesis. Epilepsy Res. (2010), doi:10.1016/j.eplepsyres.2010.02.002

International Journal of Neuroscience, 120, 99–103, 2010

ISSN 0020-7454 print / 1543-5245 online
DOI 10.3109/00207450903430208

informa
healthcare

Anti-Glutamate Receptor Antibodies in Pediatric Enteroviral Encephalitis

Hisashi Kawashima,[1] Kazunori Suzuki,[1] Gaku Yamanaka,[1] Yasuyo Kashiwagi,[1] Kouji Takekuma,[1] Masahiro Amaha,[1] and Yukitoshi Takahashi[2]

[1]*Department of Peadiatrics, Tokyo Medical University, Shinjuku-ku, Tokyo, Japan*

[2]*National Epilepsy Center, Shizuoka Institute of Epilepsy and Neurological Disorders, Shizuoka, Japan*

ABSTRACT

In order to better understand enteroviral encephalitis we investigated the clinical symptoms and several disease markers. Between 2000 and 2005 eight patients aged between 9 months and 5 years were admitted to our hospital with one case having sequela. Glutamic oxaloacetic transaminase (GOT), serum IL-6, and ferritin were elevated in most of the cases. Their IL-6 and diacron-reactive oxygen metabolites (d-ROM) in cerebral spinal fluid (CSF) were also high (86%). However, pleocytosis and high protein levels in CSF were rarely found. In viral loads of the first CSF, there were no differences between the patient with sequela and the ones without sequela. However, anti-glutamate receptor IgMδ2 was only detected in the CSF of the patient with sequela. These findings suggest that the immunological phenomenon is more closely related to the development of sequela related to enteroviral encephalitis than other disease markers, such as inflammatory cytokine, free radicals, and viral loads. Therefore, a specific therapy against immunological status might decrease the sequela; however, further research is necessary to confirm this.

KEYWORDS: anti-glutamate receptor antibodies, encephalitis, enterovirus, free radical, children, IL-6

INTRODUCTION

In 1998, there was a pandemic of encephalomyelitis accompanied with hand-foot-and-mouth disease with high mortality in Taiwan (Chang et al., 1999), and a pandemic of cerebellar ataxia accompanied with enterovirus in Japan. Recently, an increase in cases of encephalitis with enterovirus was reported in Japan. However, there are few reports about the pathophysiology and the characteristics of enterovirus-associated encephalitis. In 1999, we started to measure enterovirus RNA in cerebral spinal fluid (CSF) by using highly sensitive reverse transcription polymerase chain reaction (RT-PCR). We identified eight cases of enteroviral encephalitis. In order to choose the best treatment, we have also been measuring inflammatory cytokines, oxidative stress, viral loads, and anti-glutamate receptor antibodies in serum and CSF. In this study we investigated these disease markers and their relationship to clinical symptoms in eight patients with pediatric enteroviral encephalitis.

Address correspondence to Hisashi Kawashima, M.D., Ph.D., Department of Peadiatrics, Tokyo Medical University, 6-7-1 Nishishinjuku, Shinjuku-ku, Tokyo 160-0023, Japan.
E-mail: hisashi@tokyo-med.ac.jp

METHODS

We studied eight patients who were hospitalized due to fever, convulsions, and continuous unconsciousness. All were positive for enterovirus by RT-PCR or usual viral isolation. Their EEG showed slow wave in all the cases. Brain imaging showed abnormal findings, which revealed brain edema in five out of eight cases. The serum levels of immunoglobulin of all patients were normal.

The RT-PCR target was the consensus region of the 5′ no-coding region of the enterovirus. RNA was reverse-transcribed with avian myeloblastosis virus (AMV); reverse transcriptase using an anti-sense primer and nested PCR was also done (Takami et al., 1998). The primers of the quantitative assay were selected from the same consensus region of the 5′ no-coding region. The quantitative assay was performed by using the primers and probes, which were made

according to the sequence data of nested PCR products. The two different fluorescent oligonucleotide probes, the donor and acceptor, were designed to hybridize. The fluorescent oligonucleotide was measured by LightCycler (Roche Diagnostics GmbH, Germany) (Amaha, Kawashima, Takami, Takekuma, & Hoshika, 2006).

The oxidative status was examined by measuring the hydrogen peroxide concentration in the CSF according to the method automated by the Diacron (Diacron-Reactive Oxygen Metabolites: d-ROM test, Diacron, Italy) (Cesarone et al., 1999; Cornelli, Terranova, Luca, Cornelli, & Alberti, 2001). The serum levels of the d-ROM test ranged between 250 and 300 U.CARR (Carratelli units), where 1 U.CARR corresponds to 0.8 mg/L H_2O_2. CSF negative for enterovirus as a control was obtained from patients with fever of unknown origin, urinary tract infection, influenza, pneumonia, leukemia, and febrile seizures. The CSF levels of the d-ROM in controls were below 10 U.CARR. Serum levels of IL-6 were assayed by chemoluminescence enzyme immunoassay (CLEIA) by using Lumipulse *f* (Fujirebio Diagnostics Inc, Tokyo, Japan). We also investigated white blood cells (WBC), glutamic oxaloacetic transaminase (GOT), lactate dehydrogenase (LDH), ferritin, creatine kinase (CK), c-reactive protein (CRP), and anti-glutamate receptor antibodies. The assay of anti-glutamate receptor antibodies was examined with Western blot using Takahashi methods (Takahashi et al., 2003).

RESULTS

The patients were aged between 9 months and 5 years (two males, six females). Their symptoms before convulsion were upper respiratory tract infection in all cases (100%) and digestive symptoms in five cases (62.5%). The duration of the convulsions ranged from 2 to 60 min. One-third of the patients had asymmetric convulsions. Convulsive status was seen in six cases and a series of short convulsions in two cases. One of the eight patients (12.5%) had involuntary movements and sequela (epilepsy and paraplegia). The involuntary movements of the right upper extremity appeared 7 days after admission and resolved after several months of treatment with anti-epileptic medicines. The profiles are shown in Table 1. Blood tests showed that CRP was mildly positive in most of the cases (0.4 to 4.7 mg/dl). GOT levels were high in all the cases. Serum IL-6 was high in all the patients and ferritin in 50% of the patients. IL-6 and d-ROM in CSF were both high in 86% of the patients at the time of admission. However, pleocytosis was not found in the CSF of only one patient and the protein levels were low. In the viral loads of the CSF, there were no differences between the patient with sequela and those without sequela, similar to the levels of IL-6 and d-ROM in serum and CSF.

Anti-glutamate-receptor IgM-δ2 was detected in one out of three cases in CSF and in two out of three cases in serum. Anti-glutamate-receptor IgG-δ2 was detected in one out of three cases in serum. Anti-glutamate-receptor IgG-ε2 was positive in one out of three cases (Table 2). A patient who had anti-glutamate-receptor IgMδ2 in CSF had sequela.

DISCUSSION

We investigated eight cases, aged between 9 months and 5 years with enterovirus-associated encephalitis. Only one out of eight patients had sequela. Brain damage by neuroinfection can be caused by high inflammatory cytokines, direct viral invasion, free radicals, glutamate, apoptosis, and immunological phenomenon (Lipton, 1997). We measured the viral load, IL-6, and free radicals in this study. Leukocytosis of CSF did not appear in seven out of eight cases and appears to be likely induced later by the production of IL-6. Both IL-6 and d-ROM were high in five out of seven cases during the early stage. IL-6 is a multifunctional cytokine that plays a central role in the host defense due to its wide range of immune and hematopoietic activities and its potent ability to induce an acute-phase response. Overexpression of IL-6 has been implicated in the pathology of a number of diseases including systemic inflammatory response syndrome (SIRS) and secondary multiple organ failure (Giannoudis et al., 2008).

Recently, a new test for the evaluation of oxidative status, the d-ROM test, has become available. Although there are various reports of serum or plasma d-ROM levels (Cesarone et al., 1999; Cornelli et al., 2001), CSF d-ROM levels have not been reported. We measured d-ROM in patients with meningoencephalitis with enterovirus and 88.7% cases (6 out of 7) showed high d-ROM. CSF d-ROM in influenza-associated encephalopathy and febrile seizure has been reported (Yamanaka et al., 2006). d-ROM in CSF obtained from patients with febrile seizures was below 10 U.CARR. Yang & Qin (2004) have reported the high expression of neuronal nitric oxide synthase (nNOS) in animal models with recurrent seizures. Severe cases showed high levels in CSF and were related to the protein concentration. Oxidative stress and uncontrolled stress might influence these complications. Nitrogen oxide (NO×) inhibitors, such as a free

TABLE 1 Profiles of patients

Case	1	2	3	4	5	6	7	8
Gender	F	M	F	F	F	F	M	F
Age	1 y 5 m	9 m	1 y 1 m	10 m	9 m	10 m	3 y 9 m	5 y 10 m
Fever during illness (days)	3	4	2	2	2	2	1	2
Symptoms preceding the onset of encephalitis	Coryza diarrhea	Coryza diarrhea	Coryza	Coryza diarrhea	Coryza	Moist cough xxx syndrome	Coryza OMA abdominal pain	Coryza headache vomiting
Convulsion (minutes)	55 GTC (right side dominant)	15, 60 GTC	60 GTC (upper extremities dominant)	49 GTC (right side dominant)	15, 30 GTC	6, 60 GTC	5, 10, 3 GTC	3 GTC
Others	Choreoathetosis	-	-	-	-	-	Delirium	-
Sequela (until 1 year)	Epilepsy paraplegia	-	-	-	-	-	-	-

GTC: Generalized tonic seizure.

TABLE 2 The findings of peripheral blood and spinal fluid on admission

Case	1	2	3	4	5	6	7	8
Blood check								
CRP (mg/dl)	4.7	3.3	0.7	< 0.3	3.8	< 0.3	5.8	2.9
GOT (IU/L)	165	56	180	148	33	61	53	37
LDH (IU/L)	804	563	1029	619	575	667	521	553
CK (IU/L)	120	1510	118	240	98	730	92	203
Ferritin (mg/dl)	638	85.9	745.6	166	ND	ND	92.5	53.7
IL-6(pg/ml)	96.3	ND	51	ND	86.7	ND	126.2	ND
anti-Glu-R								
IgM-δ2	+		−		+			
IgG-δ2	+		−		−			
IgG-ε2	−		−		+			
CSF check								
Cell count	5	12	5	3	38	6	0	172
Protein (mg/dl)	12	27	13	5	12	22	9	9
Glucose (mg/dl)	85	65	90	78	80	66	85	73
IL-6 (<5 pg/ml	27.3	1.1	56.6	44	64.1	75	28.1	ND
d-ROM (<10 U.CARR)	19	39	71	17	39	59	3	ND
Viral load (copies)	937	ND	ND	ND	781	1275	ND	977
Anti-Glu-R			−					
IgM-δ2	+				−			

radical scavenger, edaravone, might be helpful in these cases.

Inoue (2002) reported NO and IL-6 production from microglia, which is activated by adenosine triphosphate (ATP) in mice. He showed that microglia stimulated by a low concentration of ATP rapidly releases plasminogen, which may protect neurons. However, microglia stimulated by a higher concentration of ATP releases TNF-α 2–3 hr after the stimulation and IL-6 6 hr after the stimulation. He speculated that stronger stimulation changes the function of microglia and induces apoptosis in neurons by releasing toxic factors, including NO (Inoue, 2002). Therefore, high NO might mean activation of microglia. High NO× was found in CSF obtained from severe influenza-associated encephalopathy (Kawashima et al., 2003). This oxidative stress might induce damage to CNS. Consequently, therapies against high cytokines and free radicals should be recommended during an acute phase of enteroviral encephalitis.

Anti-glutamate receptor antibodies are detected in the serum and CSF of patients with chronic progressive epilepsia partialis continua of childhood and those with Rasmussen's encephalitis (Takahashi et al., 2003). Moreover, these antibodies have been reported with encephalitis and encephalopathy, including limbic encephalitis without any deterioration (Kumakura, Miyajima, Fujii, Takahashi, & Ito, 2003; Takahashi, 2002). Interestingly, in our study anti-glutamate antibodies were detected in the CSF obtained from a patient with sequela. These findings suggest that the immunological phenomenon may result in sequela of enteroviral encephalitis than inflammatory cytokine, free radicals, and viral loads. The autoimmune mechanism might induce the pathophysiology of subsequent symptoms of enteroviral encephalitis. Therefore, these results suggest that therapies such as steroids, anti-virus agents, and free radical scavengers may help to prevent further sequela. However, further research with a larger number of patients is necessary to draw any definitive conclusions.

REFERENCES

Amaha, M., Kawashima, H., Takami, T., Takekuma, K., & Hoshika, A. (2006). Viral load of enterovirus in CSF by using quantitative assay and clinical symptoms. *Journal of Tokyo Medical University (Tokyo igaku zasshi)*, *64*, 361–367.

Cesarone, M. R., Belcaro, G., Carratelli, M., Cornelli, U., De Sanctis, M. T., Incandela, L., et al. (1999). A simple test to monitor oxidative stress. *International Angiology*, *18*, 127–130.

Chang, L. Y., Lin, T. Y., Hsu, K. H., Huang, Y. C., Lin, K. L., Hsueh, C., et al. (1999). Clinical features and risk factors of pulmonary oedema after enterovirus-71-related hand, foot, and mouth disease. *Lancet*, *354*(9191), 1682–1686.

Cornelli, U., Terranova, R., Luca, S., Cornelli, M., & Alberti, A. (2001). Bioavailability and antioxidant activity of some food supplements in men and women using the D-Roms test as a marker of oxidative stress. *The Journal of Nutrition*, *131*, 3208–3211.

Giannoudis, P. V., Harwood, P. J., Loughenbury, P., Van Griensven, M., Krettek, C., & Pape, H. C. (2008). Correlation between IL-6 levels and the systemic inflammatory response score: Can an IL-6 cutoff predict a SIRS state? *The Journal of Trauma*, *65*, 646–52.

Inoue, K. (2002). Microglial activation by purines and pyrimidines. *Glia*, *40*, 156–163.

Kawashima, H., Watanabe, Y., Morishima, T., Togashi, T., Yamada, N., Kashiwagi, Y., et al. (2003). NOx (nitrite/nitrate) in cerebral spinal fluids obtained from patients with influenza-associated encephalopathy. *Neuropediatrics*, *34*, 137–140.

Kumakura, A., Miyajima, T., Fujii, T., Takahashi, Y., & Ito, M. (2003). A patient with epilepsia partialis continua with anti-glutamate receptor epsilon 2 antibodies. *Pediatric Neurology, 29*, 160–163.

Lipton, S. A. (1997). Neuropathogenesis of acquired immunodeficiency syndrome dementia. *Current Opinion in Neurology, 10*, 247–253.

Takahashi, Y. (2002). Anti-Glu R ε antibodies in intractable epilepsy after CNS infection in children. *Journal of Japan Pediatric Society, 106*, 1402–1411.

Takahashi, Y., Mori, H., Mishina, M., Watanabe, M., Fujiwara, T., Shimomura, J., et al. (2003). Autoantibodies to NMDA receptor in patients with chronic forms of epilepsia partialis continua. *Neurology, 61*, 891–896.

Takami, T., Kawashima, H., Takei, Y., et al. (1998). Usefulness of nested PCR and sequence analysis in a nosocomial outbreak of neonatal enterovirus infection. *Journal of Clinical Virology, 11*, 67–75.

Yamanaka, G., Kawashima, H., Suganami, Y., Watanabe, C., Watanabe, Y., Miyajima, T., et al. (2006). Diagnostic and predictive value of cerebrospinal fluid d-ROM levels in patients with influenza-associated encephalopathy. *Journal of the Neurological Sciences, 243*, 71–75.

Yang, Z. X., & Qin, J. (2004). Interaction between endogenous nitric oxide and carbon monoxide in the pathogenesis of recurrent febrile seizures. *Biochemical Biophysics Research Communications, 315*, 349–355.

INTERNAL MEDICINE

□ EDITORIAL □

Can We Predict a Prolonged Course and Intractable Cases of Herpes Simplex Encephalitis?

Hiroshi Shoji

Key words: herpes simplex encephalitis, acyclovir, prognostic factor

(Inter Med 48: 177-178, 2009)
(DOI: 10.2169/internalmedicine.48.1737)

In Japan, herpes simplex encephalitis (HSE) has historically been fatal in approximately 30% of all reported cases. After the induction of acyclovir (ACV), however, the mortality rate has decreased to 7.1% (1), and HSE is now regarded as a treatable disease. However, the rate of poor outcome including moderate or severe sequelae still remains at 30-40% of HSE patients, despite standard ACV treatment. It is conceivable that early detection and appropriate treatment will lead to a good prognosis for intractable HSE.

Problems in prolonged and intractable cases of HSE were taken up at the workshop held by the Japan Herpesvirus Infections Forum (JHIF) in 1996 (2) and the symposium of the Japanese Neuro-Infectious Disease Meeting in 1997 (unpublished data). At that time, a tentative definition of intractable cases of HSE was developed as follows:

1. Cases of HSE that develop to an apallic state and to fatality.

2. Prolonged cases that require more than 6 months' hospitalization.

3. Recurrent cases.

It may be that the main reasons for the development of intractable HSE are a deep consciousness disturbance, status epilepticus, and delays in starting antiviral drug therapy. Conventionally in the USA, a semicoma or coma state in patients over 30 years of age has been accepted as a predictive factor in a fatal prognosis (3).

In this issue of the journal (see also pp 89-94), Taira et al (4) analyzed variable predictors such as age, sex, Glasgo coma scale (GCS), starting date of ACV, corticosteroid administration, and cranial computed tomography (CT), as well as magnetic resonance imaging or electroencephalogram abnormalities between the prolonged group (n=8) and non-prolonged group (n=15) in 23 adult HSE patients. The prolonged group was defined as being without any neurological improvement at the time of completion of ACV treatment for 14 days, and they concluded that there are 2 significant predictors of a prolonged course of HSE; a lower GCS $\leqq$6 points at the start of antiviral treatment and a higher rate of abnormal lesion on initial CT. The 4 patients of the prolonged group had poor outcomes at 3 months after onset.

The clinical guidelines for adult HSE in Japan recommend a higher dose of ACV for severe HSE patients and alternative therapy of vidarabine in unresponsive cases to ACV treatment (5). A recent study also suggests that corticosteroid administration is a beneficial factor for HSE prognosis (6). Therefore, when HSE patients present with GCS $\leqq$6 points and CT abnormal lesion on the temporal lobe, it seems likely that we should initiate ACV treatment at a higher dosage (45-60 mg/day), or add corticosteroid administration including pulse therapy.

However, the pathophysiology for these 2 predictors should be clarified. Intractable cases with a deep consciousness disturbance or wide CT abnormality are often attributed to prolonged herpes simplex virus (HSV) infection or secondary encephalitis (postinfectious/autoimmune encephalitis). Further virologic and immunologic studies are expected to investigate the use of real-time polymerase chain reaction for HSV DNA, and changes of various cytokines in the host response.

References

1. Ohtani S, Kogure H, Sekizawa T, et al. Therapeutic effect of acyclovir on herpes simplex virus encephalitis・meningitis. Rinshou To Virus **11**: 282-295, 1983 (in Japanese).
2. JHIF Workshop on the diagnosis and treatment of herpes simplex encephalitis (HSE), and intractable HSE cases. Shoji H, Ed. Churchill Communications Jpn, Tokyo, 1997: 7-30 (in Japanese).
3. Whitley RJ, Alford CA, Hirsch MS, et al. Vidarabine versus acyclovir therapy in herpes simplex encephalitis. N Engl J Med **314**:

Fukuoka School of Rehabilitation Sciences, International University of Health and Welfare, Okawa
Correspondence to Dr. Hiroshi Shoji, hshoji@iuhw.ac.jp

144-149, 1986.
4. Taira N, Kamei S, Morita A, et al. Predictors of prolonged clinical course in adult patients with herpes simplex virus encephalitis. Intern Med **48**: 89-94, 2009.
5. Japanese Society for Neuroinfectious Diseases, Ed. Clinical guideline of herpes simplex encephalitis. Neuroinfection **10**: 78-87, 2005 (in Japanese).
6. Kamei S, Sekizawa T, Shiota H, et al. Evaluation of combination therapy using both aciclovir and corticosteroid in adult patients with herpes simplex virus encephalitis. J Neurol Neurosurg Psychiatry **76**: 1544-1549, 2005.

BRAIN RESEARCH 1250 (2009) 233–241

available at www.sciencedirect.com

ScienceDirect

www.elsevier.com/locate/brainres

BRAIN RESEARCH

Research Report

Motor impairment and aberrant production of neurochemicals in human α-synuclein A30P+A53T transgenic mice with α-synuclein pathology☆

Masaki Ikeda[a], *Takeshi Kawarabayashi*[b], *Yasuo Harigaya*[d], *Atsushi Sasaki*[c], *Shuichi Yamada*[g], *Etsuro Matsubara*[e], *Tetsuro Murakami*[f], *Yuya Tanaka*[f], *Tomoko Kurata*[f], *Xu Wuhua*[f], *Kenji Ueda*[h], *Hisashi Kuribara*[i], *Yasushi Ikarashi*[j], *Yoichi Nakazato*[c], *Koichi Okamoto*[a], *Koji Abe*[f], *Mikio Shoji*[b,*]

[a]*Department of Neurology, Gunma University Graduate School of Medicine, Maebashi, Japan*
[b]*Department of Neurology, Hirosaki University School of Medicine, Hirosaki, Japan*
[c]*Department of Human Pathology, Gunma University Graduate School of Medicine, Maebashi, Japan*
[d]*Department of Neurology, Maebashi Red Cross Hospital, Maebashi, Gunma, Japan*
[e]*Department of Alzheimer's Disease Research, National Institute for Longevity Sciences, Obu, Japan*
[f]*Department of Neurology, Neuroscience, Biophysiological Science, Okayama University Graduate School of Medicine and Dentistry, Okayama, Japan*
[g]*Immuno-Biological Laboratories Co., Ltd., Mikasa, Hokkaidio, Japan*
[h]*Department of Neural Plasticity, Tokyo Institute of Psychiatry, Setagaya-ku, Tokyo, Japan*
[i]*Tokyo University of Social Welfare, Isesaki, Japan*
[j]*R and D Division, Tsumura and Co., Ltd, Inashiki, Japan*

ARTICLE INFO

Article history:
Accepted 6 October 2008
Available online 1 November 2008

Keywords:
α-synuclein
Mutation
Transgenic mouse
Parkinson's disease
Neurochemical

ABSTRACT

Missense point mutations, duplication and triplication in the α-synuclein (αSYN) gene have been identified in familial Parkinson's disease (PD). Familial and sporadic PD show common pathological features of αSYN pathologies, e.g., Lewy bodies (LBs) and Lewy neurites (LNs), and a loss of dopaminergic neurons in the substantia nigra that leads to motor disturbances. To elucidate the mechanism of αSYN pathologies, we generated TgαSYN transgenic mice overexpressing human αSYN with double mutations in A30P and A53T. Human αSYN accumulated widely in neurons, processes and aberrant neuronal inclusion bodies. Sarcosyl-insoluble αSYN, as well as phosphorylated, ubiquitinated and nitrated αSYN, was accumulated in the brains. Significantly decreased levels of dopamine (DA) were recognized in the striatum. Motor impairment was revealed in a rotarod test. Thus, TgαSYN is a useful model for analyzing the pathological cascade from aggregated αSYN to motor disturbance, and may be useful for drug trials.

☆ Grant numbers and sources of supports: Supported by **Grant-in-Aid for** Grants-in-Aid for Primary Amyloidosis Research Committee (M. S.), from the Ministry of Health, Labor and Welfare of Japan and by Grants-in-Aid for Scientific Research (B) (M.S.: 19390233, K.A.: 18390257), (C) (M.I.: 19590980, T.K.: 19590976, A.S.: 18500276, E.M.: 18590968), from the Ministry of Education, Culture, Sports, Science and Technology, Japan.

* *Corresponding author.* Fax: +81 172 39 5143.
E-mail address: mshoji@hirosaki-u.ac.jp (M. Shoji).

0006-8993/$ – see front matter © 2008 Published by Elsevier B.V.
doi:10.1016/j.brainres.2008.10.011

1. Introduction

αSYN was originally isolated from senile plaques in Alzheimer's disease as a protein of 35 highly hydrophobic amino acid metabolites, known as the non-amyloid component (NAC), derived from a 140 amino-acid precursor encoded by a gene on chromosome 4 (Ueda et al., 1992; Chen et al., 1995), which has homology to rat and Torpedo αSYN and songbird synelfin (George et al., 1995). αSYN is highly abundant in presynaptic terminals (Iwai et al., 1995) and has potential roles in synaptic function and neural plasticity (George et al., 1995; Clayton and George, 1998).αSYN binds to phospholipid vesicles and inhibits PLD2, a regulator of vesicle membrane budding (Liscovitch et al., 2000; Lotharius and Brundin, 2000; Payton et al., 2000), and also plays modulatory roles in the release of dopamine vesicles (Abeliovich et al., 2000).

A few cases of familial Parkinson's disease (FPD) have been linked to missense point mutations in αSYN with A53T (Polymeropoulos et al., 1997), A30P (Kruger et al., 1998) and E46K (PARK1) (Zarranz et al., 2004). Soon after the first A53T missense mutation of αSYN was discovered, the main component of Lewy bodies (LBs) was identified as insoluble aggregates of αSYN (Baba et al., 1998). αSYN and phosphorylated-Ser129 αSYN accumulated in LBs and Lewy neurites (LNs) in PD and Dementia with Lewy bodies (DLB) (Fujiwara et al., 2002; Hasegawa et al., 2002). Then, a second causative gene known as *parkin* (Kitada et al., 1998) was found in familial autosomal recessive juvenile Parkinson's disease (PARK2). *Parkin* ubiquitinates αSYN normally and this process is aberrantly altered in PD (Shimura et al., 2001). Acceleration of oligomerization or protofibrillization is a common property of mutant αSYN (Conway et al., 2001; Choi et al., 2004). Recently, triplication of the αSYN locus (PARK4) was identified in an "Iowanian kindred" with autosomal dominant Lewy body disease (Singleton et al., 2002). Subsequently, duplication of the αSYN gene locus was also reported as a cause of familial PD (Chartier-Harlin et al., 2004). These findings suggest that overexpression of wild type αSYN also leads to facilitation of insoluble aggregation of αSYN. α-synucleinopathy is a disease entity which shares common pathological accumulation of insoluble aggregates of αSYN in the neurons and processes of PD, DLB, Hallervorden–Spatz disease, pure autonomic failure and in the glial cells of multiple system atrophy (MSA) (Goedert, 2000; Hardy and Gwinn-Hardy, 1998; Spillantini et al., 1997; Tu et al., 1998; Galvin et al., 2000; Shoji et al., 2000; Arai et al., 2000).

To elucidate the pathological mechanism of LBs and LNs associated with the decrease in dopamine (DA) production, it is necessary to investigate the aberrant mechanism of mutant αSYN, which is an essential molecule consisting of LBs and LNs (Baba et al., 1998). Here, we generated transgenic (Tg) mice expressing human mutant αSYN A30P+A53T under a human Thy-1 promoter, named as TgαSYN. Overexpression of double mutant human αSYN was expected to lead to further synergistic effects and induce severe α-synucleinopathies and neurodegeneration (Citron et al., 1998; Chishti et al., 2001). TgαSYN showed significant motor impairment in rotarod test, accumulation of insoluble αSYN, aberrant inclusions and decreased dopamine levels. These findings indicate that TgαSYN is a useful animal model to investigate the crucial pathogenesis of α-synucleinopathies, and it may help to develop therapeutic agents.

2. Results

2.1. *Expression of αSYN in transgenic mice and analyses of RT-PCR*

We used the transgene construct hThy1-αSYN A30P+A53T to generate transgenic (Tg) mice, TgαSYN (Fig. 1a). PCR analysis of tail-derived DNA revealed 18 positive Tg mice for human αSYN and EGFP among 129 F0 mice. Five of the 18 Tg mice showed the strongest green fluorescence under irradiation at 365 nm ultraviolet (Fig. 1b). These selected independent lines (#8707, #8713, #8718, #8812, #8819) were mated with BDF1 mice and raised for examination. The following Tg mice were analyzed: 18 positive Tg progenies, 60 F1 Tg (#8707: 2, #8713: 31, #8718: 5, #8812: 10, #8819: 12) and 135 F2 Tg (#8707: 0, #8713: 101, #8718: 2, #8812: 29, #8819: 3). The mRNA expressions of human αSYN A30P+A53T and EGFP in TgαSYN brains were confirmed by RT-PCR, showing the same expression levels of human αSYN A30P+A53T and EGFP at three, eight and 17 months old, respectively (Figs. 1c and d). Western blot using LB509 recognized a 16 kD band corresponding to human αSYN only in Tg mice. AB5038 recognized a 16 kD band corresponding to both human and mouse αSYN. The expression level of human αSYN was 130% of that of endogenous mouse αSYN (Fig. 1e).

2.2. *Histological studies*

Immunocytochemistry of sagittal sections of a seven-month-old #8707 TgαSYN brain by LB509 revealed extensive human αSYN immunostaining in the brainstem, hippocampus, thalamus, cerebral cortex and cerebellum (Fig. 2a, arrow indicates the substantia nigra), but no staining in the non-Tg mouse (Fig. 2b). The TgαSYN brain showed atrophy of the cerebral cortex and cerebellum (Fig. 2a). The HE stain showed eosinophilic inclusion bodies and vacuoles in the cytoplasm of neurons in the substantia nigra (Fig. 2c, arrow), and in the dentate nucleus of TgαSYN (Fig. 2h, arrow). These cytoplasmic inclusions were stained with human-αSYN specific antibody, LB509 (Fig. 2d, arrow, and Fig. 2i, arrow), and anti-αSYN antibody, 42/α-Synuclein (Fig. 2j, arrows). Nitrated α/β synuclein was also stained in the cytoplasmic inclusions (Fig. 2e, arrow,). Ubiquitin-positive inclusions were observed in neurons at brainstem (Fig. 2f, arrow), and dystrophic neurites in the dentate nucleus of TgαSYN (Fig. 2g). Staining of phosphorylated synuclein showed diffuse staining in somatodendrites of TgαSYN neurons (Fig. 2k). Gallyas–Braak staining revealed dystrophic neurites in the dentate nucleus of TgαSYN (Fig. 2l) in ubiquitin-positive structures in the same region (Fig. 2g). Anti-tyrosine hydroxylase (TH) immuno-positive neurons in the locus ceruleus showed weak immunostaining intensity in TgαSYN (Fig. 2m), compared with those of non-Tg mice brains (Fig. 2n). The intensity of substance P immunopositive synapses in the striata of TgαSYN brains (Fig. 2o) was weaker than that of non-Tg mice brains (Fig. 2p). Severe astrocytosis

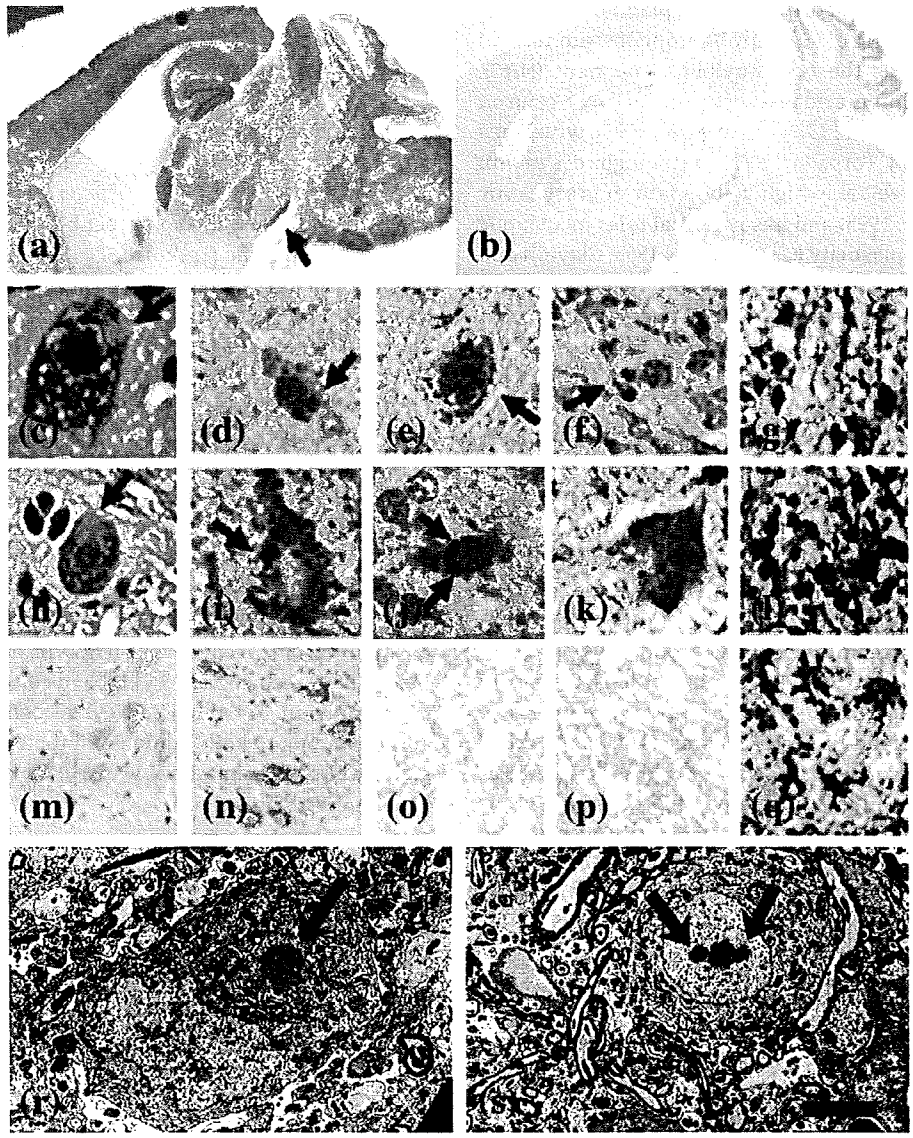

Fig. 2 – The pathological features of TgαSYN at seven months of age and age-matched non-Tg mice. (a) A sagittal section of a seven-month-old #8707 TgαSYN brain labeled by LB509 showed extensive αSYN accumulation prominently in the brainstem, hippocampus, thalamus, cerebellum and cerebral cortex. The substantia nigra of the midbrain is also labeled (arrow). The cerebral cortex and cerebellum showed atrophy. (b) No staining in the non-Tg mice brain by LB509. (c) Hematoxylin–eosin stain showed eosinophilic inclusion bodies and vacuoles in the cytoplasm of neurons in the substantia nigra of #8707 TgαSYN (arrow). (d) LB509 detected cytoplasmic inclusions in the substantia nigra of #8707 TgαSYN (arrow). (e) Anti-nitrated α/β SYN monoclonal antibody (Syn12) immunostained cytoplasmic inclusions in the substantia nigra (arrow), as well as in 14-month-old #8713 TgαSYN. (f) Ubiquitin-positive inclusions are shown in the substantia nigra of #8707 TgαSYN (arrow). (g) Ubiquitin-positive dystrophic neurites in the cerebellum dentate of 16-month-old #8713 TgαSYN. (h) Eosinophilic cytoplasmic inclusions (arrow) in the dentate nucleus of #8707 TgαSYN. (i) LB509-positive inclusion in the dentate nucleus of #8707 TgαSYN (arrow). (j) Cytoplasmic inclusions immunostained with a mouse monoclonal antibody 42/α-Synuclein in the brainstem of #8812 TgαSYN (arrow). (k) The PSer129 αSYN antibody immunostained the cytoplasm of neurons in the substantia nigra of #8707 TgαSYN. (l) Gallyas–Braak stain of dystrophic neurites in the dentate nucleus of a 16-month-old #8713 TgαSYN. (m) Tyrosine hydroxylase (TH) immuno-positive neurons in the locus ceruleus showed less immunostaining in the #8707 TgαSYN brain, than the non-Tg mouse brain (n). (o) The intensity of substance P immuno-positive synapses in the striatum of #8707 TgαSYN brain was lower than non-Tg mice brain (p). (q) Astrocytosis in the cerebellum of 16-month-old #8713 TgαSYN. (r) Electron-dense inclusions were found in the cytoplasm of neurons in the brainstems of 8-month-old #8718 TgαSYN by an EM study (arrow). (s) In the brainstem of the same mouse, intracellular inclusions (arrows) were also detected. Scale bar = 1 mm in a, b, 12.5 μm in c–f, h–k, 50 μm in g, l, m, n, 25 μm in o, p, and 0.38 μm in r, s.

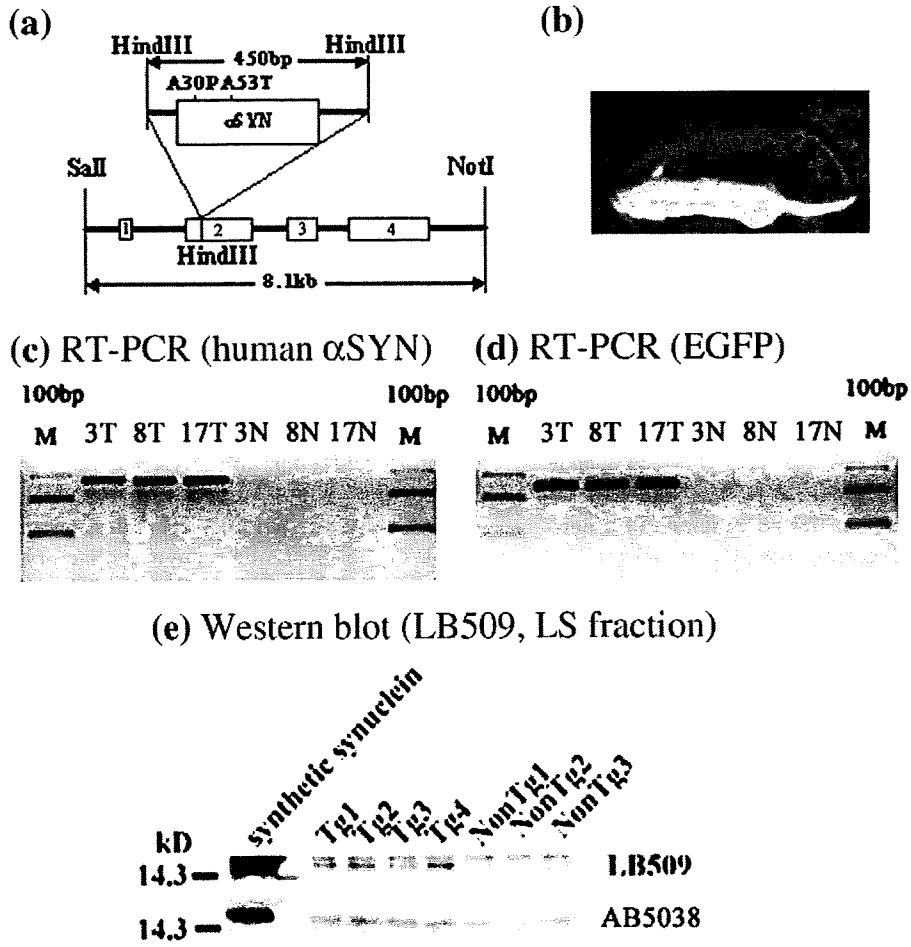

Fig. 1–The mutant αSYN A30P+A53T construct and the expression of EGFP. (a) The structure of the construct: hThy1-αSYN A30P+A53T. (b) TgαSYN (#8713) showed fluorescence by EGFP (enhanced green fluorescence protein) under 365 nm long wave UV (EGFP-negative non-Tg mouse in the upper location, EGFP-positive Tg mouse in the lower location). (c) Analyses of RT-PCR transcripts: Human αSYN mRNA transcripts (exons 2–4) were detected as 280 bp in TgαSYN brains, but not in non-Tg mice brains, and the intensity of PCR products was the same level as three-, eight-, and 17-month-old Tg mice brains. (d) EGFP mRNA transcripts were detected in TgαSYN brains at the same level at three, eight and 17 months of age, but not in non-Tg mice brains (N showed non-Tg mice brains, T showed Tg mice brains). (e) The expression of human αSYN was detected as a 16 kD band at the same size as recombinant synthetic αSYN by Western blot using LB509 in LS-soluble fractions of TgαSYN #8713 (Tg1–4) mice brains, but not in three 14-month-old non-Tg mice brains (upper lane). AB5038 recognized a 16 kD band corresponding to human and mouse αSYN (lower lane). The expression level of human αSYN was about 130% of that of endogenous mouse αSYN. Synthetic αSYN (SS) was used as a marker of 16 kD αSYN (BIOMOL Research Laboratories Inc., Plymouth Meeting, PA).

was observed in the cerebellum of a 16-month-old TgαSYN (Fig. 2q). An EM study demonstrated cytoplasmic inclusions (Fig. 2r, arrow) and intranuclear inclusions (Fig. 2s, arrows) in the neurons of the brainstem. These inclusion bodies lacked the typical halo and fibrillar structure of LBs.

2.3. *Western blot analysis*

Fourteen-month-old TgαSYN showed a 16 kD band corresponding to αSYN in the LS-soluble fraction (L), Triton-soluble fraction (T), sarcosyl-soluble (S) and sarcosyl-insoluble fractions (I) (Fig. 3a: arrow). In sarcosyl-insoluble fraction, smear pattern was detected in TgαSYN#8812(T3), which accumulated much synuclein histologically. The anti-phosphorylated αSYN antibody pSyn#64 labeled the same size band as αSYN, 16 kD (Fig. 3b: arrow). These findings presented that sarcosyl-insoluble human αSYN and phosphorylated αSYN was accumulated in TgαSYN brains as reported in DLB brains (Hasegawa et al., 2002).

2.4. *Rotarod test for motor function of TgαSYN*

The rotarod test demonstrated that significant motor impairment appeared after a shorter time in TgαSYN; they dropped from the rotating rod faster than non-Tg littermates. The motor impairment was found at three months of age ($p<0.01$) and thereafter deteriorated with age ($p<0.001$. Fig. 4).

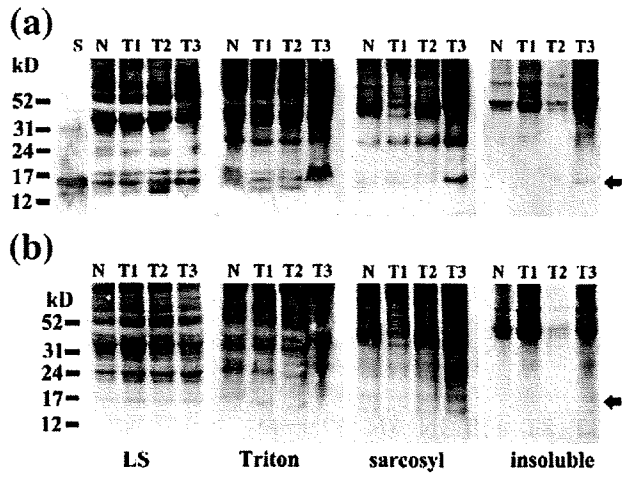

Fig. 3–Western blot analysis. The expression of human αSYN was 16 kD (lane S; corresponded to recombinant human αSYN) by Western blot using antibody LB509 (a) and pSyn#64 (b) in LS-soluble (L), Triton-soluble (T), sarcosyl-soluble (S) and sarcosyl-insoluble (I) fractions of non-Tg (N), TgαSYN#8713 (T1), TgαSYN#8819 (T2), and TgαSYN#8812 (T3), 14-month-old mice brains.

2.5. *Measurement of neurochemicals*

There was no significant difference in brain weight among Tg and non-Tg mice at 10 and 17 months of age. Compared with age-matched non-Tg control mice, the levels of DA in the striatum were significantly decreased in 10 month-old (p=0.0159) and 17 month-old mice brains (p=0.0286). DA decreased approximately 17% to 24% in the striatum of TgαSYN brains (Fig. 5a). A significant decrease in DA was also detected in the hypothalamuses of 17-month-old TgαSYN brains (p=0.0079. Fig. 5b). NE was not decreased in any areas of 10-month-old TgαSYN brains (Fig. 5c). Serotonin was decreased in the hypothalamuses of 10- and 17-month-old TgαSYN brains (p=0.0079, p=0.0286, respectively. Fig. 5d). ACh decreased in the striatum in 17-month-old TgαSYN (p=0.0286. Fig. 5e). There was no significant alteration in DOPAC, HVA, MHPG, 5-HIAA and Ch levels in any areas of TgαSYN (data not shown). These results showed that insoluble mutant αSYN aggregation selectively decreased the DA level at 10 and 17 months of age.

3. Discussion

Several groups have already reported animal models of PD, such as wild-type αSYN Tg mice (Masliah et al., 2000), mutant αSYN Tg mice (van der Putten et al., 2000, Kahle et al., 2000, Giasson et al., 2002, Lee et al., 2002, Richfield et al., 2002, Neumann et al., 2002, Thiruchelvam et al., 2004, Tofaris et al. 2006, Wakamatsu et al., 2008), *Drosophila melanogaster* (Pendleton et al., 2002) and *C. elegans* (Kuwahara et al., 2006). The first αSYN Tg mice expressed wild-type human αSYN driven by the PDGF-β promoter (Masliah et al., 2000). This mouse displayed intraneuronal inclusions immunoreactive for αSYN and ubiquitin in several regions typically affected in α-synucleinopathies, while lacking the characteristic fibrillar components of Lewy bodies. The Tg mice overexpressing αSYN A53T developed under the murine Thy-1 regulatory sequence showed an early and dramatic decline in motor function (van der Putten et al., 2000). Transgenic wild-type and A30P αSYN abnormally accumulated in neuronal cell bodies and neurites throughout the brain (Kahle et al., 2000). Mice expressing wild-type or A53T αSYN under the mouse prion promoter developed motor deficits by eight months of age (Giasson et al., 2002). Neuropathological assessment of these Tg mice revealed a wide distribution of αSYN, with a pathological sparing of the motor cortex and a total sparing of the substantia nigra. Another group developed Tg mice harboring αSYN A53T using a mouse prion promoter showing motor dysfunction and αSYN accumulation (Lee et al., 2002). Truncated human αSYN (C-120) Tg mice under the TH promoter led to pathological changes in dopaminergic nerve cells of the substantia nigra and olfactory bulb (Tofaris et al., 2006). Recently, truncated human αSYN (C-130) Tg mice also led to selective loss of dopaminergic neurons and accumulation of phosphorylated αSYN (Wakamatsu et al., 2007, 2008).

One of the differences between these models and our TgαSYN was a novel combination of a promoter and mutation of αSYN. TgαSYN expressed double mutant αSYN with A30P +A53T under the human Thy-1 promoter. As expected, our TgαSYN demonstrated widespread αSYN accumulation in the brainstem, caudate putamen, cerebellum, hippocampus and cerebral cortex. Eosinophilic inclusion bodies in the substantia nigra and dentate nucleus of the cerebellum corresponded to accumulation of αSYN. Accumulated αSYN was ubiquitinated, nitrated and phosphorylated at the histological levels as shown in PD and DLB brain. Unfortunately, these inclusion bodies were not compatible with typical LBs because of the absence of a halo structure. At the EM level, fibrillar structure was not observed in inclusion bodies, but they were composed of massive aberrant fine granular structures. Aberrant inclusion bodies with modified αSYN were also observed widely. Since Gallyas–Braak staining labeled these LNs, accumulated αSYN in these neurites may have characteristics of those in β-sheet pleated structures.

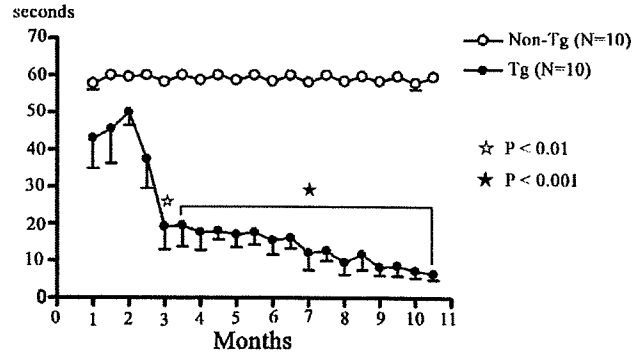

Fig. 4–Rotarod test. The retention time of Tg mice on the rotarod significantly decreased in TgαSYN. The significant difference began to decrease at three months old (☆: p<0.01) and progressively deteriorated in an age-dependent manner from six months (★: p<0.001). Statistics were analyzed by two-way repeated measures ANOVA.

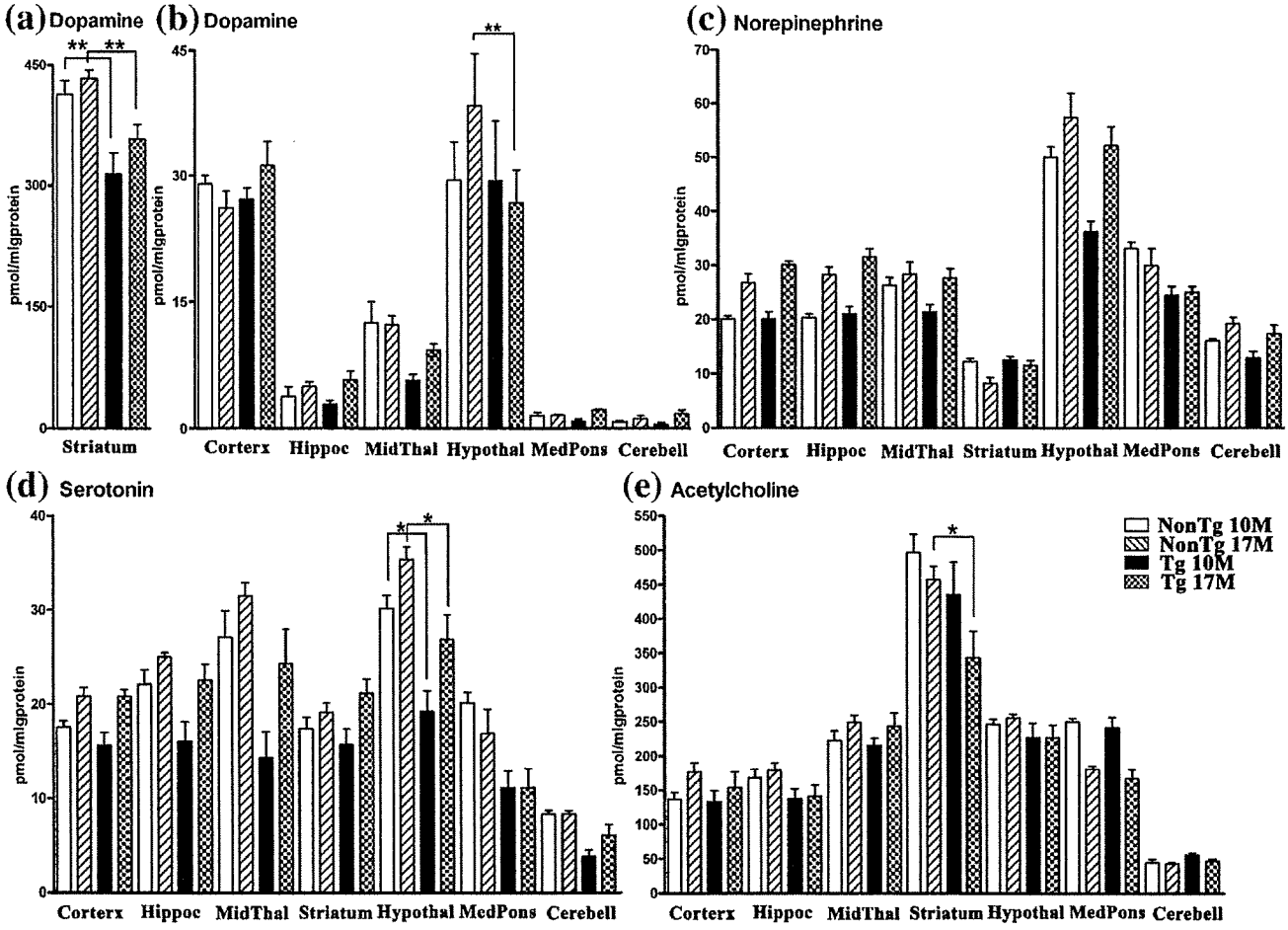

Fig. 5 – Measurement of neurochemicals. Opened column: 10-month-old non-Tg mice, Oblique column: 17-month-old non-Tg mice; Closed black colored column: 10-month-old TgαSYN mice, Crossed column: 17-month-old non-Tg mice. Cortex: cerebral cortex, Hippoc: hippocampus, MidThal: midbrain–thalamus, Hypothal: hypothalamus, MedPons: medulla–pons, Cerebell: cerebellum. *$p<0.01$, **$p<0.05$. Statistical analysis of neurochemicals between the TgαSYN and non-Tg control groups at the same age was conducted by a two-way repeated measure ANOVA (GraphPad Prism 4). (a) DA was significantly decreased in the striatum in 10- and 17-month-old TgαSYN compared with non-Tg control mice. (b) A decrease in dopamine was detected significantly in the hypothalamuses of 17-month-old TgαSYN brains ($p=0.0079$). (c) Norepinephrine (NE) was not decreased in 10- and 17-month-old TgαSYN brains. (d) Serotonin (5-HT) was decreased in the hypothalamus of 10- and 17-month-old TgαSYN brains ($p=0.0079$, $p=0.0286$, respectively). (e) ACh was decreased in the striatum of 17-month-old TgαSYN ($p=0.0286$).

The α-synuclein pathologies in TgαSYN were accompanied by decreased tyrosine hydroxylase-positive neurons, Substance P synapses and severe astrocytosis. These histological α-synuclein pathologies were also detected at the biochemical level. Accumulated αSYN was phosphorylated, ubiquitinated and sarcosyl-insoluble, suggesting that it may be conformationally changed as reported in PD/DLB brains (Hasegawa et al., 2002). The presence of higher molecule phosphorylated and ubiquitinated bands (22/29 kD) on Western blots also indicated that accumulated αSYN was modified and aggregated.

The severe decrease in DA and loss of dopaminergic neurons in SNc and the striata of PD brains is widely believed to be the pathological and biochemical cause of PD. Notably, our TgαSYN demonstrated decreased DA production in a disturbed DA system which was measured in the liquid chromatographic systems. Although other neurochemicals were altered slightly, a prominently decreased level of DA was revealed in the striatum of TgαSYN. These findings suggest selective neurotoxicity with αSYN accumulation.

In our mouse model, approximately a 20% reduction in DA in the striatum was observed when motor impairment existed. Since the rotarod test revealed significant decreased spontaneous movement, the phenotype of TgαSYN is quite similar to the cardinal clinical symptom of PD, akinesia. A decreased level of TH-positive neurons and substance P synapses also suggested that the motor impairment in TgαSYN may be caused by aberrant αSYN processes.

Our TgαSYN is a mammalian model animal showing decreased DA and motor deficits, which were certainly detected by the liquid chromatographic systems and rotarod test. For this reason, TgαSYN is a useful model for analyzing the aberrant cascade induced by pathological metabolism and aggregation of mutant αSYN, and may be useful for developing essential treatments for α-synucleinopathies such as PD and DLB.

4. Experimental procedures

4.1. *Transgene construction, generation of transgenic mice and analyses of RT-PCR*

Human αSYN A30P+A53T cDNA (450 bp) was ligated into Hind III sites in the human Thy-1 genome gene. The transgene hThy1-αSYN A30P+A53T consisted of an 8.1 kb XhoI–NcoI fragment of pBluescript II KS kidney enhancer (Fig. 1a). The CX-EGFP transgene consisted of a 3 kb Xba I/BamH I fragment of pCAGGS containing the CMV enhancer, β-actin promoter, a part of the rabbit β-globin gene, a part of the second intron, the third exon and 3′-untranslated region and cDNA of EGFP (Enhanced green fluorescent protein) with the Kozak sequence (Imai et al., 1999). Approximately 2,000 copies of the transgene with a 1:1 mole rate mixture of the hThy1-αSYN A30P+A53T and CX-EGFP as a transgene marker were micro-injected into the pronuclei of fertilized BDF1 eggs. To analyze gene expression of human αSYN, RT-PCR was performed using 2 μl of mRNA, isolated using the QuickPrep Micro mRNA purification kit (GE Healthcare Bio-Sciences Corp., Piscataway, NJ), from the brains of TgαSYN (#8713) and non-Tg mice brains at 3, 8, 17 months of age ($n=3$, respectively) in the reaction tube of Ready-To-Go RT-PCR Beads (GE Healthcare Bio-Sciences Corp., Piscataway, NJ) with PCR primer sets as follows: (αSYN forward primer: TG GAT GTA TTC ATG AAA GGA, αSYN reverse primer: CC AGT GGC TGC TGC AAT GCT C; EGFP forward primer: TGG TGA GCA AGG GCG AGG AG; EGFP reverse primer: TCG TGC TGC TTC ATG TGG TC). For semi-quantification, RT-PCR of β-actin was performed as an internal control (Elliott, 2001). Ten microliters of PCR products were analyzed by 2.5% agarose gel electrophoresis. The intensity of ethidium-stained bands was analyzed by Scion Image (Scion Corporation, Frederick, MD).

4.2. *Histological examinations*

After mice were sacrificed under anesthesia, the brains were removed and cut sagittally along the midline. One hemisphere was fixed in 0.1 mol/L phosphate buffer (PB, pH 7.6) containing 4% paraformaldehyde, and embedded in paraffin. For immunostaining, 5-μm sections were treated with 99% formic acid for 3 min, or treated in a microwave at 500 W for 5 min three times in 10 mmol/L citrate buffer (pH 6.0). After blocking with 5% normal goat or horse serum in 50 mmol/L phosphate buffered saline (PBS) containing 0.05% Tween-20 and 4% Block-Ace (Snow brand, Sapporo, Japan), sections were incubated with primary antibodies for 6 h. Specific labeling was visualized using a Vectastain Elite ABC kit (Vector, Burlingame, CA). Immunostained tissue sections were counterstained with hematoxylin. Nissl, Hematoxylin–eosin (H–E), and Gallyas–Braak stains were also done.

The following antibodies were used: mouse monoclonal antibody to human αSYN, LB509 (×4, residues 115–121/122) (Baba et al., 1998); mouse monoclonal antibody to αSYN, 42/α-Synuclein (×50, BD Transduction Laboratories, San Jose, CA); rabbit polyclonal antibody to phosphorylated Serine at residue 129 of human αSYN, PSer129 (×200) (Fujiwara et al., 2002; Hasegawa et al., 2002); rabbit polyclonal antibody to tyrosine hydroxylase (TH), AB151 (×2,000, CHEMICON, Temecula, CA); rabbit polyclonal antibody to substance P, AB1566 (×1,000, CHEMICON, Temecula, CA); rabbit polyclonal antibody to ubiquitin, UbiQ (×500) (Ikeda et al., 2005; Murakami et al., 2006); mouse monoclonal antibody to nitrated α/β SYN, Syn12 (×400, Invitrogen, Corps., Carlsbad, CA); rabbit polyclonal antibody to glial fibrillary acidic protein (GFAP, ×20,000, DAKO, Carpinteria, CA).

For electron microscopic (EM) studies, the brain tissues were immersed in a fixative solution (2.5% glutaraldehyde, 0.1 mol/L phosphate buffer (PB), pH 7.4) for 4 h and washed several times in 0.1 mol/L PB containing 7% sucrose. Blocks were then postfixed in 2% osmium tetroxide, dehydrated in ethanol and propylene oxide, and embedded in Quetol 812 (Nisshin EM, Tokyo, Japan). Ultrathin sections were stained with uranyl acetate and lead acetate prior to observation.

4.3. *Western blot analysis*

Half of each brain was homogenized in 3 ml/g of low-salt buffer (LS: 10 mmol/L Tris, 5 mmol/L ethylenediaminetetraacetic acid (EDTA), 1 mmol/L dithiothreitol (DTT), 10% sucrose, and a cocktail of protease inhibitors (Complete®, Roche Diagnostics, Indianapolis, IN), pH 7.5) and centrifuged at 25,000 g for 30 min at 4 °C (LS-soluble fraction). Pellets were treated with 3 ml/g of LS with 1% Triton X-100 and 0.5 mol/L NaCl, and centrifuged at 180,000 g for 30 min at 4 °C (Triton-soluble fraction). Pellets were then homogenized again in 2 ml/g LS with 1% N-lauroylsarcosine (SIGMA CHEMICAL CO. St Louis, MO) and 0.5 mol/L NaCl, incubated at 22 °C on a shaker for 1 h, and centrifuged at 180,000 g for 30 min at 22 °C. Supernatants were analyzed as sarcosyl-soluble fraction (Iwatsubo et al., 1996; Hasegawa et al., 2002; Sampathu et al., 2003; Ikeda et al., 2005; Murakami et al., 2006). The remaining pellets obtained from each sarcosyl-insoluble fraction were boiled at 70 °C in 20 μl of NuPAGE® LDS Sample Buffer for 10 min. Each fraction was separated on 4 to 12% NuPAGE Bis–Tris Gels (Invitrogen, Corps., Carlsbad, CA) and the blots were labeled by a mouse monoclonal antibody to human αSYN (LB509, ×4), and a mouse monoclonal antibody to phosphorylated Serine at residue 129 of human αSYN (pSyn#64, ×200, Wako, Japan). Signals were visualized with an enhanced chemiluminescence detection system (SuperSignal West® Dura Extended Duration Substrate, PIERCE, Rockford, IL) and quantified by a luminoimage analyzer (LAS 1000-mini, Fuji film, Tokyo, Japan).

4.4. *Measurement of neurochemicals*

Neurochemicals, including dopaminergic (dopamine: DA, 3,4-dihydroxyphenylacetic acid: DOPAC, homovanillic acid: HVA), noradrenergic (norepinephrine: NE, 3-methoxy-4hydroxyphenylglycol: MHPG), serotonergic (5-hydroxytryptamine: 5-HT, 5-hydroxyindoleacetic acid: 5-HIAA) and cholinergic (acetylcholine: ACh, choline: Ch) systems in the brain were measured in Tg mice ($n=10$) and non-Tg control mice ($n=10$) at 10 and 17 months old, respectively. In brief, each animal was anesthetized with Nembutal® (Dainippon Pharmaceutical Co. Ltd., pentobarbital sodium), sacrificed, and irradiated with microwaves (NJE 2603 Microwave device, New Japan Radio, Kamifukuoka, Japan) at 9.0 kW for 0.42 s to prevent post-mortem

changes in the neurochemicals during brain sampling (Ikarashi et al., 1985, 2004). The brain was removed from the skull and dissected into seven regions (cerebral cortex, hippocampus, midbrain–thalamus, striatum, hypothalamus, medulla–pons and cerebellum) according to the established method (Glowinski and Iversen, 1966), and then each region was weighed. Each dissected brain region was homogenized with 0.5 ml of 0.1 mol/L perchloric acid containing 0.8 nmol isoproterenol hydrochloride as an internal standard for the determinations of catecholamines, indoleamines and related metabolites, and 5 nmol ethylhomocholine iodide as an internal standard for the determinations of ACh and Ch, using an ultrasonic cell disrupter (US-300T, Nissei, Tokyo, Japan). The homogenate was centrifuged at 17,300 g at 4 °C for 15 min. The supernatant was filtered through a 0.45 μm millipore filter. Aliquots, typically 10 μl of the filtrates, were injected into the liquid chromatographic systems (Eicom HPLC-ECD system, Eicom Co. Ltd., Kyoto, Japan) to determine catecholamines-, indoleamines-, and acetylcholine-related substances (Ikarashi et al., 1992). The sediment was re-homogenized with 2 ml of 1 mol/L NaOH for a protein assay, which was performed using the method of Lowry et al. (1951). The concentrations of neurochemicals in the brain were expressed as the values per milligram of protein.

4.5. *Behavioral experiments*

4.5.1. *Rotarod test*

TgαSYN (n=10) and age-matched control mice (n=10) at one month to 10.5 months old were examined by the rotarod performance test according to a previous method (Kuribara et al., 1977; Ikarashi et al., 2004). Mice were placed on the rotating rod of the apparatus (Ugo basile, biological research apparatus, Milan, Italy) at a speed of 16 rpm for 300 s, and the time they stayed on the rotating rod was measured. Each set of three trials was performed at 10 minute intervals each day for every mouse.

4.6. *Statistical analyses*

Two-way repeated measures ANOVA followed by the Mann–Whitney U test for the rotarod test and open field test, and two-way ANOVA followed by Student's t test to analyze neurochemicals were performed using GraphPad Prism 4 (GraphPad Software Inc., San Diego, CA) and SPSS 10.0 (SPSS 10.0 for Windows, SPSS Inc., Chicago, IL). The means of all data are presented with their standard errors (mean±S.E.).

Acknowledgments

We thank Dr. T Iwatsubo for coordinative provision of the LB 509 antibody and polyclonal phosphorylated αSYN antibody, Dr. D Dickson for the antibody Ubi-Q and Dr. S Kawabata for the human Thy-1 gene. We thank Dr. H Sugimoto and Dr. T Izumi for technical supports, and Dr. J Hirato for kind coordinative support. We also thank Y Nogami and H Narihiro for technical assistance. All animal experiments were performed according to guidelines established in the "Guide for the Care and Use of Laboratory Animals" (Japan).

REFERENCES

Abeliovich, A., Schmitz, Y., Farinas, I., Choi-Lundberg, D., Ho, W.H., Castillo, P.E., Shinsky, N., Verdugo, J.M., Armanini, M., Ryan, A., Hynes, M., Phillips, H., Sulzer, D., Rosenthal, A., 2000. Mice lacking α-synuclein display functional deficits in the nigrostriataL-DOPAmine system. Neuron 25, 239–252.

Arai, K., Kato, N., Kashiwado, K., Hattori, T., 2000. Pure autonomic failure in association with human α-synucleinopathy. Neurosci. Lett. 296, 171–173.

Baba, M., Nakajo, S., Tu, P.H., Tomita, T., Nakaya, K., Lee, V.M., Trojanowski, J.Q., Iwatsubo, T., 1998. Aggregation of α-synuclein in Lewy bodies of sporadic Parkinson's disease and dementia with Lewy bodies. Am. J. Pathol. 152, 879–884.

Chartier-Harlin, M.C., Kachergus, J., Roumier, C., Mouroux, V., Douay, X., Lincoln, S., Levecque, C., Larvor, L., Andrieux, J., Hulihan, M., Waucquier, N., Defebvre, L., Amouyel, P., Farrer, M., Destée, A., 2004. -Synuclein locus duplication as a cause of familial Parkinson's disease. Lancet 364, 1167–1169.

Chen, X., de Silva, H.A., Pettenati, M.J., Rao, P.N., St. George-Hyslop, P., Roses, A.D., Xia, Y., Horsburgh, K., Ueda, K., Saitoh, T., 1995. The human NACP/α-synuclein gene: chromosome assignment to 4q21.3–q22 and TaqI RFLP analysis. Genomics 26, 425–427.

Chishti, M.A., Yang, D.S., Janus, C., Phinney, A.L., Horne, P., Pearson, J., Strome, R., Zuker, N., Loukides, J., French, J., Turner, S., Lozza, G., Grilli, M., Kunicki, S., Morissette, C., Paquette, J., Gervais, F., Bergeron, C., Fraser, P.E., Carlson, G.A., George-Hyslop, P.S., Westaway, D., 2001. Early-onset amyloid deposition and cognitive deficits in transgenic mice expressing a double mutant form of amyloid precursor protein 695. J. Biol. Chem. 276, 21562–21570.

Choi, W., Zibaee, S., Goedert, M., 2004. Mutation increases phospholipids binding and assembly into filaments of human α-synuclein. FEBS Lett. 576, 363–368.

Citron, M., Eckman, C.B., Diehl, T.S., Corcoran, C., Ostaszewski, B. L., Xia, W., Levesque, G., St. George-Hyslop, P., Younkin, S.G., Selkoe, D.J., 1998. Additive effects of PS1 and APP mutations on secretion of the 42-residue amyloid β-protein. Neurobiol. Dis. 5, 107–116.

Clayton, D.F., George, J.M., 1998. The synucleins: a family of proteins involved in synaptic function, plasticity, neurodegeneration and disease. Trends. Neurosci. 21, 249–254.

Conway, K.A., Rochet, J.C., Bieganski, R.M., Lansbury Jr., P.T., 2001. Kinetic stabilization of the α-synuclein protofibril by a dopamine-α-synuclein adduct. Science 294, 1346–1349.

Elliott, J.L., 2001. Cytokine upregulation in a murine model of familial amyotrophic lateral sclerosis. Brain Res. Mol. Brain Res. 95, 172–178.

Fujiwara, H., Hasegawa, M., Dohmae, N., Kawashima, A., Masliah, E., Goldberg, M.S., Shen, J., Takio, K., Iwatsubo, T., 2002. -Synuclein is phosphorylated in synucleinopathy lesions. Nat. Cell Biol. 4, 160–164.

Galvin, J.E., Giasson, B., Hurtig, H.I., Lee, V.M., Trojanowski, J.Q., 2000. Neurodegeneration with brain iron accumulation, type 1 is characterized by α-, β-, and γ-synuclein neuropathology. Am. J. Pathol. 157, 361–368.

George, J.M., Jin, H., Woods, W.S., Clayton, D.F., 1995. Characterization of a novel protein regulated during the critical period for song learning in the zebra finch. Neuron 15, 361–372.

Giasson, B.I., Duda, J.E., Quinn, S.M., Zhang, B., Trojanowski, J.Q., Lee, V.M., 2002. Neuronal α-Synucleinopathy with severe movement disorder in mice expressing A53T human α-synuclein. Neuron 34, 521–533.

Glowinski, J., Iversen, L.L., 1966. Regional studies of catecholamines in the rat brain. I. The disposition of [^{3}H]norepinephrine, [^{3}H]dopamine and [^{3}H]dopa in various regions of the brain. J. Neurochem. 13, 655–669.